J Water Environ Nanotechnol 2026, 11(3): 420-430
10.22090/jwent.2026.2076641.1997

RESEARCH PAPER

Phytochemical Synthesis and Application of Aluminum Oxide Nanoparticles in Photocatalytic Oxidation of Ametryn

Kavya Bekkalale Madegowda**, Thimmaiah Mahadevaiah

Department of Civil Engineering, BGS Institute of Technology, Adichunchanagiri University, Mandya, Karnataka – 571 448, India

*Corresponding Author(s)
Email:
kavyadarpan26@gmail.com

Article History:

Received: 2025-11-03
Revised: 2026-01-25
Accepted: 2026-02-03

How to cite this article
Kavya BM and Mahadevaih T. Phytochemical Synthesis and Application of Aluminum Oxide Nanoparticles in Photocatalytic Oxidation of Ametryn. J Water Environ Nanotechnol 2026, 11(3): 420-430, DOI: 10.22090/jwent.2026.2076641.1997

HIGHLIGHTS

- Eco-friendly synthesis of Al_2O_3 nanoparticles using Hibiscus rosa-sinensis leaf extract.
- Increased leaching of the herbicide ametryn was observed in soils with high pH and low organic matter.
- Achieved 84.0% ametryn removal and a 74.2% COD reduction under UV illumination.
- Maximum photocatalytic activity was recorded under acidic conditions (pH 3) with a catalyst loading of 2.5 g/L.
- The synthesized nanoparticles demonstrated good stability and were successfully reused for up to five consecutive cycles

ABSTRACT

The present study investigates the phytochemical synthesis of aluminium oxide nanoparticles (Al_2O_3 NPs) using *Hibiscus rosa-sinensis* leaf extract and their application in the photocatalytic oxidation of ametryn, a herbicide commonly used in sugarcane cultivation. Column studies were conducted to assess the leaching of ametryn through soil, revealing increased mobility in soils with low organic matter content and higher pH. On characterization of synthesized nanoparticles, SEM images revealed agglomerated spherical structures with smooth surfaces, while XRD analysis confirmed the presence of aluminium oxide with a face-centred cubic structure. FTIR results indicated the presence of various functional groups on the surface of the Al_2O_3 NPs, potentially contributing to their stability and biocompatibility. The photocatalytic degradation of ametryn was studied under UV illumination, with Al_2O_3 NPs as the catalyst. The effects of catalyst dosage, pH, and initial herbicide concentration on the degradation efficiency were investigated. The highest removal efficiency of 84.0% was achieved with a catalyst loading of 2.5 g/L at pH 3, with 74.2% of COD reduction. Increasing the catalyst dosage from 0.5 g/L to 3.0 g/L enhanced the degradation efficiency by 17%. The process was found to be more effective under acidic conditions, with a notable reduction in degradation efficacy of 7.6% as pH increased from 2.5 to 4.0. Reusability studies showed that the catalyst could be used for up to five consecutive cycles, with a 37% reduction in degradation efficiency. Kinetic studies revealed that the pseudo-first-order rate kinetic model fit the process.

KEYWORDS:

Hibiscus Rosa-sinesis; Photocatalytic Oxidation; Nanoparticles; Aluminium Nanoparticles; Herbicides; Ametryn

©2026 The Author(s). Published by the Iranian Environmental Mutagen Society. This work is licensed under the Creative Commons Attribution 4.0 International License (CC BY 4.0). To view a copy of this license, visit http://creativecommons.org/licenses/by/4.0/.

1. INTRODUCTION

Sugarcane as a high-value crop contributes substantially to the economies of many tropical and subtropical countries. With specific climatic conditions including warm temperatures, abundant sunlight, and adequate rainfall or irrigation, sugarcane has a long growing cycle, typically 12-18 months, which allows for extensive root development, which aids in soil conservation and nutrient uptake. Weed infestation poses a significant challenge in sugarcane cultivation, potentially leading to substantial yield losses and reduced crop quality. These unwanted plants compete with sugarcane for essential resources such as water, nutrients, and sunlight, hindering the crop's growth and development. The weed problem is most pronounced during the early growth stages of sugarcane, a period when the crop is highly susceptible to the competitive pressure from weeds. Common weed species in sugarcane fields include grasses, sedges, and broadleaf weeds, each presenting unique management challenges. Herbicide application, while effective, requires careful consideration to prevent environmental impacts and the development of herbicide-resistant weed populations. Integrated weed management approaches, incorporating crop rotation, timely cultivation, and appropriate herbicide use, are crucial for sustainable sugarcane production and long-term weed control.

Ametryn, a selective herbicide belonging to the triazine group, has vital application in sugarcane farming as it effectively manages broadleaf weeds and grasses. Ametryn offers targeted weed control, eliminating unwanted plants while sparing sugarcane crops. By removing weeds, it lessens the competition for water, nutrients, and sunlight, thereby enhancing the yield and quality of sugarcane. When applied to sugarcane fields, ametryn may not be fully absorbed by the target plants or soil. Intense rainfall or irrigation can remove herbicides that have not been absorbed from the soil surface, leading to their entry into nearby water bodies. Furthermore, soil erosion can carry soil particles contaminated with ametryn into streams and rivers. The herbicide's moderate solubility in water and its persistence in the environment enhance its movement in runoff. The degree to which ametryn is washed off is influenced by factors such as the dose of ametryn applied, the characteristics of the soil, the landscape, and prevailing weather conditions [1].

Acayaba et al (2020) reported 1101 ng/L ametryn and other herbicides from the largest agricultural runoff in Brazil. The monitoring included 30 active ingredients of pesticides, with 2-hydroxy atrazine, diuron, carbendazim, tebuthiuron, and hexazinone being among the most frequently detected. In another work, Silva and co-workers (2016) conducted column studies in which ametryn was applied to a sugarcane crop and 60 mm rainfall was simulated after draining the column. The study reported that ametryn mobility was influenced by organic content, texture, and cation exchange capacity. According to a 2022 study, 80% of surface water samples from agricultural regions in Brazil contained ametryn, with concentrations up to 1.2 μg/L. The researchers observed that even low concentrations can have detrimental effects on aquatic organisms and lead to the contamination of water sources. Ametryn has a half-life of up to 120 days in soil and can leach into groundwater.

The suitability of chemical treatment method Fenton and Photo-Fenton oxidation, Sono-chemical treatment, electrochemical oxidation, and photocatalytic oxidation, for organic contaminants has been demonstrated by various researchers due to their recalcitrant nature for biological treatment [2-5]. Over the past few years, there has been substantial advancement in Advanced Oxidation Processes (AOPs), particularly in tackling effluents from textile herbicides and other stubborn pollutants. Notable improvements have occurred in the field of catalyst engineering, with the creation of novel materials such as titanium dioxide nanoparticles with dopants and composite structures. These innovations have demonstrated improved effectiveness in decomposing complex herbicide molecules [6], [7], [8]. Photocatalytic oxidation is a process that uses light energy to activate a catalyst, which then facilitates the oxidation of various substances. Common photocatalysts include titanium dioxide (TiO_2), zinc oxide (ZnO), and various metal oxides [9-11].

Davarpanah and team (2015) synthesized magnetite nanoparticles via a novel co-precipitation method that demonstrated high affinity for removing p-toluic acid (Davarpanah et al., 2015). In another study of the adsorption process, diethanolamine-functionalized polystyrene resin (DEA-PS) efficiently removes p-toluenesulfonic acid (p-TSA).

The field of photocatalytic oxidation has witnessed the rise of aluminium nanoparticles as compelling alternatives to traditional photocatalysts. These nanoscale materials exhibit exceptional characteristics that make them particularly suitable for such applications. Notably, aluminium nanoparticles possess a significantly enhanced surface-to-volume ratio in comparison to their bulk material counterparts. This attribute translates to an increased number of catalytically active sites, potentially boosting the efficiency of oxidation reactions. Aluminium nanoparticles exhibit localised surface plasmon resonance in the ultraviolet region, thereby enhancing light absorption and photocatalytic activity. In another photocatalytic study, metal nanoparticles (Au, Ag, Pt) were deposited on TiO2 via a UV-switchable polyoxometalate intermediate to create nanohybrids with reduced bandgap energies and enhanced photocatalytic degradation of reactive blue 19 dye under UV–visible light, with Pt@PW-TiO_2 showing the highest efficiency and reaction rate.

The present approach of nanoparticle synthesis of aluminium nanoparticles using *Hibiscus rosa-sinesis* leaf extract as a catalyst precursor contrasts with conventional chemical or physical

synthesis methods, offering a sustainable, cost-effective, and biocompatible alternative. The study addresses a specific gap by applying these green-synthesized Al_2O_3 NPs as photo catalysts for the degradation of ametryn, and demonstrating catalyst reusability up to five cycles with quantified efficiency loss adds practical value for sustainable water treatment applications.

2 MATERIAL AND METHODS

2.1 Column studies of ametryn leaching

Agricultural plots were modelled using PVC columns measuring 10 cm in diameter and 50 cm in length, divided into 10 layers with 5 cm depth intervals. The columns, lined with paraffin to prevent water from draining sideways, were filled with soil. Herbicides were applied to the top of the columns at a rate of 3 kg/ha for weed management, utilizing precision spraying equipment. The columns were then subjected to simulated rainfall events to mimic natural precipitation patterns. Soil samples were collected from each layer at regular intervals to analyze herbicide distribution and movement throughout the column. Rain simulation was conducted twelve hours after the herbicide was applied, while the columns remained upright. Following the rain simulation, the columns were kept upright for an additional 72 hours to allow water to drain into the soil, and the runoff was collected and analyzed for ametryn concentration. The results of this study provided valuable insights into the vertical migration of herbicides in agricultural soils, informing best practices for herbicide application and environmental risk assessment.

2.2 Preparation of Hibiscus rosa-sinesis leaf extracts

100 grams of fresh *Hibiscus rosa-sinensis* leaves were collected, washed in distilled water to remove particulate matter, ground into a fine paste, and then heated to 80°C for approximately 1 hour. The resulting solution was filtered using Whatman's filter paper (#42) and stored at 4°C for subsequent use. The extract was filtered and stored for further use at 4 °C.

2.3 Phytochemical synthesis of Aluminum oxide nanoparticles

The green synthesis of aluminium oxide nanoparticles was conducted utilising *Hibiscus rosa-sinensis* leaf extract and aluminium chloride as a precursor. *Hibiscus rosa-sinensis* extracts were added to the 0.5 M $AlCl_3{\cdot}6H_2O$ solution and extracted dropwise until the colour transformed to black. The solutions were filtered with Whatman's No.1 filter paper and desiccated in an oven. The extracted particles were stored in moisture-free containers. The morphology, mineral composition, and chemical composition of aluminium nanoparticles were characterised using scanning electron microscopy, X-ray diffraction, and electron diffusion spectroscopic spectrophotometry, respectively.

2.4 Photocatalytic oxidation of Ametryn using Aluminium Oxide Nanoparticles

Photocatalytic degradation of ametryn using aluminium oxide nanoparticles as a catalyst was carried out with 5 mg/L of initial herbicide concentration (considering an average of leaching) [12], [13], [14]. The experiment employed illumination at a wavelength of 470 nm, with a light intensity of 5.6 mW/cm^2 at the centre of the reaction mixture. Aluminium oxide nanoparticles were added at an incremental dose into the Ametryn solution in a conical flask. The investigation was conducted with appropriate experimental conditions by considering different dosages of nanocomposite particles (0.5 g/L – 3.0 g/L). The concentration of ametryn was measured using a double-beam UV -vis spectrophotometer at the wavelength of 554 nm (Systronics Make, Model No. AU-2701) (Hou and Yin, 2011). Chemical oxygen demand (COD) was measured by the colourimetric method as per 5220D of Standard Methods for Examination of Water and Wastewater (APHA Method 4500-F, 1992). pH was measured using a digital pH meter (Model - edge, HANNA make). A recoverability and reuse test for the spent catalyst was conducted. Aluminium oxide Nanoparticles powder was filtered, collected, dried, and reused as a catalyst for the photocatalytic degradation of ametryn.

3. RESULTS AND DISCUSSION

3.1 Leaching of Ametryn through soil column

The herbicide exhibits moderate mobility, with the study soil contributing to the movement of ametryn within the soil profile. It is observed increased mobility of ametryn in soils characterized by low organic matter content. Furthermore, Silva et al. (2012) found that an increase in soil pH may reduce the sorption capacity of ametryn, leading to greater leaching of this compound within the soil profile. This occurs because when the soil pH is near or below the pKa of the herbicide, the molecule may become protonated, acquire a positive charge, and be absorbed by plants as a cation. The ametryn concentration found in the leachate is given in Fig. 1. It is observed that ametryn leaching is increased with time, contributing to its solubility in water from 1.5 mg/L to 3.8 mg/L within five days.

3.2 Synthesis of Aluminium oxide Nanoparticles formation and its characterization

Nanoparticles obtained by treating leaf extract and aluminium chloride solution were seen as agglomerated spherical structures with smooth surfaces under a Scanning Electron Microscope. Fig. 2 presents the SEM images of synthesized fresh and treated aluminium oxide nanoparticles. Five Peaks observed with XRD (Fig. 3) are at 2Θ 38.39, 44.64, 65.03, 78.43, and 82.38, representing aluminium oxide (PDF: 01-080-0956) with a face-centered cubic structure of aluminium. Four sharp peaks in the analysis indicate the degree of crystallinity of the nanoparticles.

J Water Environ Nanotechnol, 2026, 11(3): 420-430
10.22090/jwent.2026.2076641.1997

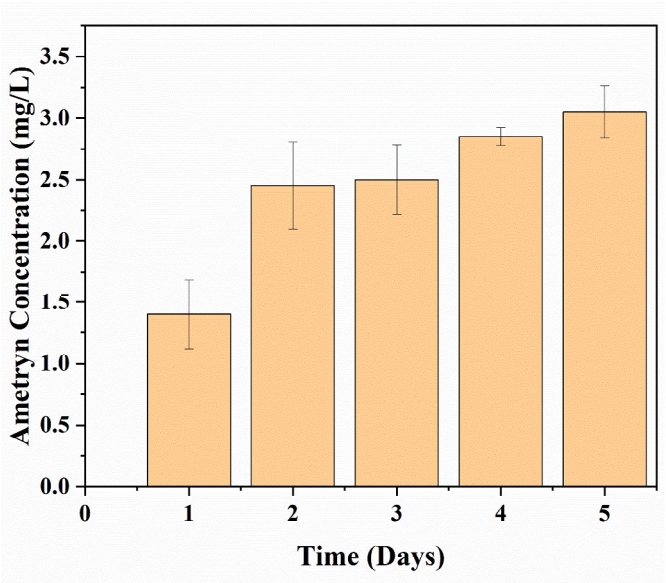

Fig. 1. Concentration of ametryn in soil leachate

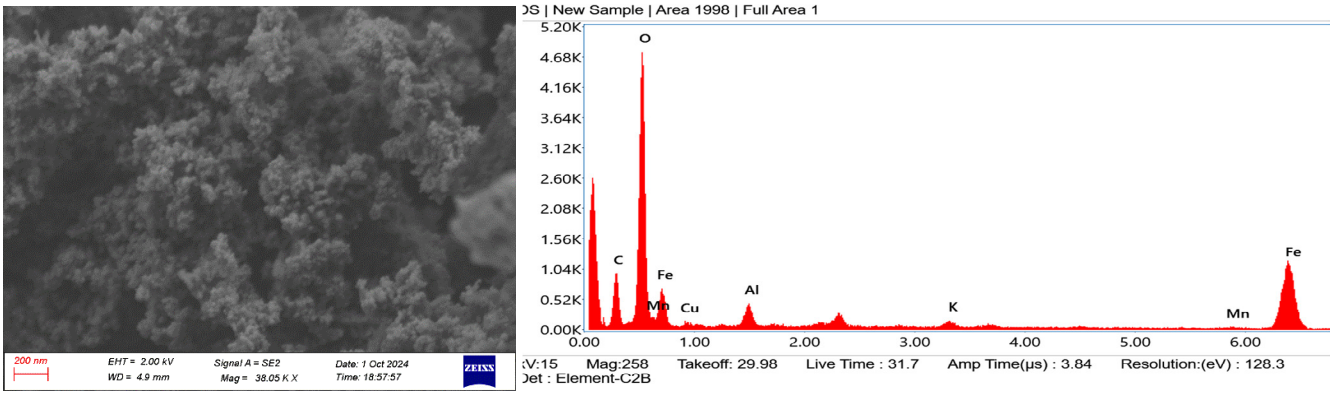

Fig. 2. Scanning Electron Microscopic images showing the morphological appearance of synthesized nanoparticles. a) Fresh nanoparticles and b) Treated nanoparticles

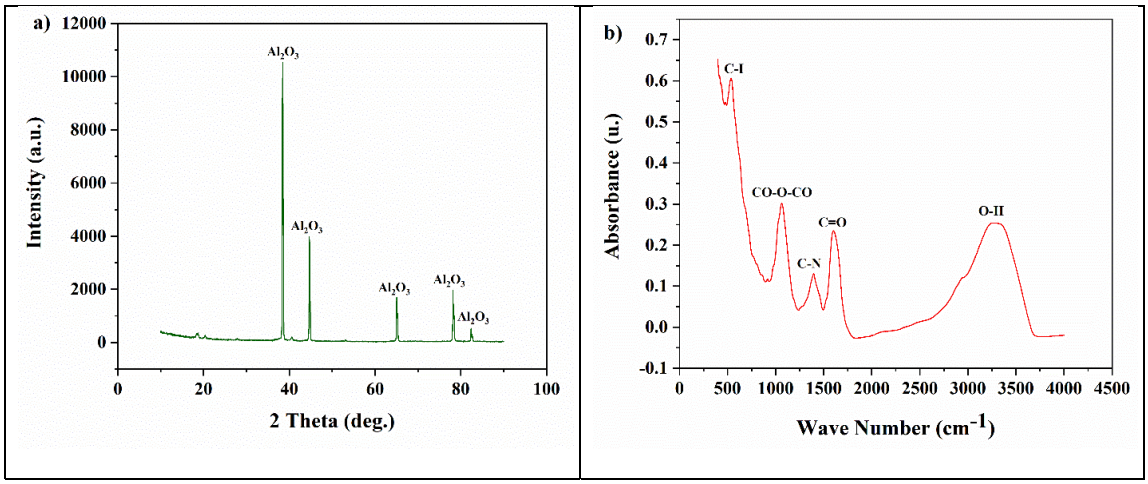

Fig. 3. a) XRD Images representing the corresponding peaks and b) BET adsorption isotherm of synthesized nanoparticles

Table 1 presents the chemical elements by weight percentage for aluminium oxide nanoparticles, with aluminium being 1.6% of total weight.

BET analysis suggests that the nitrogen adsorption data comprised 11 adsorption points with no corresponding desorption points, indicating that the analysis focused on the adsorption branch of the isotherm. The presence of pores around 39.6 nm indicates a mesoporous structure. The average pore diameter calculated using a slit pore model was 14.542 nm, suggesting some heterogeneity in pore shape or size distribution and also supporting mesoporosity, though the difference in pore size values suggests some distribution or shape variation (Fig. 3b).

The FTIR results for fresh nanoparticles indicate the presence of an inorganic aluminium compound. The bands detected near 700 to 900 cm^{-1} are predominantly attributed to the stretching vibrations of Al–O bonds. These vibrations occur in the distinct coordination environments of aluminum ions, namely octahedral and tetrahedral sites, which are common in various polymorphic forms of aluminum oxide. Peaks within the 500–700 cm^{-1} range are commonly linked to Al–O bending modes or lattice vibrations. Peaks appearing in the lower segment of this region, between 500 and 700 cm^{-1}, are generally associated with bending modes of the Al–O bonds or collective lattice vibrations. These bending vibrations reflect the flexibility and dynamics of the oxide lattice and can be indicative of the degree of crystallinity or the presence of structural defects within the nanoparticles (Fig. 4a).

For FTIR results with nanoparticles treated with ametryn, peaks confirm the retention of the core nanoparticle structure after treatment, indicating that the aluminum oxide framework remains intact and stable. Peaks in the range 1000–1500 cm^{-1} include C–N stretching vibrations associated with amine groups, C–O stretching from ether or alcohol groups, and C=C stretching from aromatic or unsaturated carbon bonds. The appearance or enhancement of peaks related to these functional groups in the FTIR spectrum of the treated nanoparticles indicates the successful adsorption or binding of ametryn onto the aluminum oxide surface. This suggests that the organic molecules are chemically or physically attached to the nanoparticle surface rather than merely being physically mixed. The peak at 1750 cm^{-1} corresponds to vibrational modes associated with carbonyl groups (C=O) and related functional groups. The carbonyl groups in ametryn may interact with the aluminum oxide surface, forming coordination bonds or hydrogen bonds, which shift or enhance the C=O stretching

Table 1. Chemical composition of synthesized Aluminum oxide nanoparticles

Elements	C	O	Fe	K	Mn	Al	Cu
Weight (%)	26.2	36.7	32.8	0.6	0.5	1.6	1.6

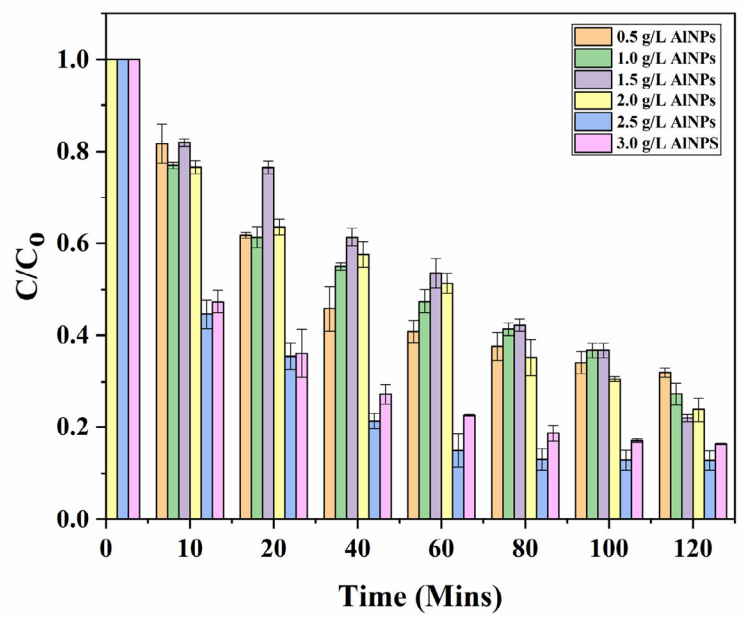

Fig. 4. FTIR spectra representing the corresponding peaks of a) Fresh nanoparticles and b) Treated nanoparticles

J Water Environ Nanotechnol, 2026, 11(3): 420-430
10.22090/jwent.2026.2076641.1997

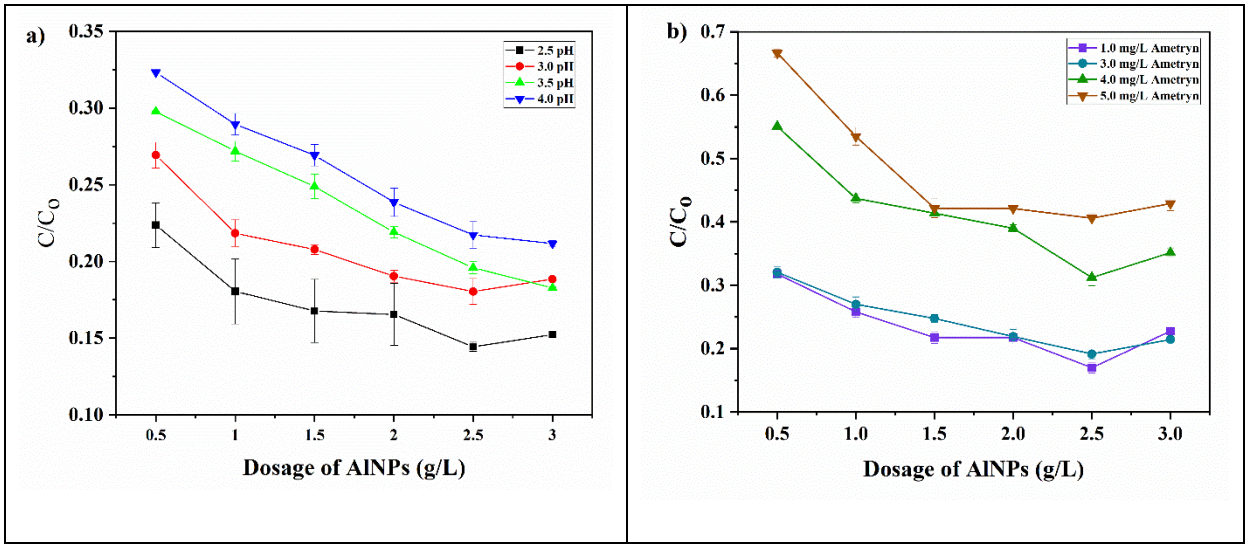

Fig. 5. Degradation of ametryn with different dosages of $Al_{2O3\ NPs}$

vibration observed in this spectral range. Appearance of new peaks in the untreated aluminum oxide may reflect the nature and strength of the interaction between ametryn and the aluminum oxide nanoparticles (Fig. 4b). The zeta potential value of -25.9 mV for the synthesized chemical indicates that the particles possess a moderately stable negative surface charge in the dispersion medium. This negative charge suggests electrostatic repulsion between particles, which helps prevent aggregation and promotes colloidal stability. The value obtained implies moderate stability, indicating the synthesized chemical is likely to remain dispersed but may be somewhat susceptible to aggregation under certain conditions.

3.3 Photocatalytic degradation of Ametryn by Aluminium Nanoparticles formation

Photocatalytic Degradation of ametryn under UV illumination with aluminium oxide nanoparticles as a catalyst was investigated. Overall removal efficiency up to 84.0% was observed with 0.0431/Min on nanoparticle loading of 2.5 g/L, pH 3, out of which 80.0% removal was observed in an initial 40 minutes and is attributed to the generation of more hydroxyl radicals due to photoexcitation (Fig. 5). The effect of catalyst dosage was studied by increasing nanoparticle dosage in the range of 0.5 g/L to 3.0 g/L. During the study, the degradation of RhB increased with an increase in the load of the catalyst. The efficiency of herbicide removal was observed to increase by 17% on increasing catalyst dosage from 0.5 g/L to 3.0 g/L. Degradation efficiency increased by 3.68% on an increase in catalyst dosage from 0.5 g/L to 1.0mg/L, 10.21% on an increase in catalyst dosage from 0.5 g/L to 1.5 g/L, and 10.78% on an increase in catalyst dosage from 0.5 g/L to 2.0 g/L, indicating the role of the catalyst in the oxidation of ametryn. This observation indicates the role of nanoparticles as a catalyst in the process of generating reactive hydroxyl radicals, thereby accelerating the formation of active sites on the catalyst. The increased catalyst dosage led to a higher concentration of active sites, resulting in more efficient herbicide degradation.

Fig. 5 (a) depicts the influence of pH on the degradation of ametryn. In the present study, the degradation of herbicides is observed to be high at pH 2.5 and 3.0, comparatively marking the suitability of acidic conditions for photocatalytic degradation. It is observed that for a catalyst loading of 2.5g/L, the observed degradation was 85.4%, 83.0%, 80.2%, and 77.8%, with a notable reduction in degradation efficacy of 7.6% as pH rises. A similar trend of degradation efficiency was observed with an increase in catalyst dosage from 0.5 g/L to 2.5 g/L at both pH 2.5 and pH 4.0, with a removal efficiency difference of 9%. The increase in degradation efficiency at pH 2.5 and 3.0 is attributed to electrostatic interactions between the herbicide molecules and the catalyst surface, which contribute to adsorption mechanisms and the generation of more hydroxyl radicals at acidic pH. The influence of initial ametryn concentration is shown in Fig. 5 (b). The study reveals that increasing the initial concentration from 5 mg/L to 20 mg/L, whilst maintaining a catalyst dosage of 2.5 g/L, results in a 23.5% decrease in degradation efficiency. Conversely, when the initial ametryn concentration is kept at 5 mg/L, raising the catalyst dosage from 0.5 g/L to 2.5 g/L enhances the degradation efficiency by 13.2%. At an initial ametryn concentration of 20 mg/L, the same increase in catalyst dosage improves degradation by 26%. Notably, the overall removal efficiency is superior at the lower initial concentration of 5 mg/L. This trend suggests that the catalyst's effectiveness is more pronounced at lower initial concentrations of ametryn.

The inverse relationship between initial concentration and degradation efficiency could be attributed to the limited availability of active sites on the catalyst surface. As the initial concentration increases, these active sites may become saturated, leading to a decrease in the overall degradation rate. Kiran Kumar Anna et al. (2022) investigated the catalytic role of aluminium nanoparticles in the photocatalytic degradation of methylene blue herbicides. The investigation employed two distinct nanoparticle synthesis methods: precipitation and sol-gel. The findings revealed that aluminium nanoparticles fabricated via the precipitation technique exhibited superior catalytic efficacy compared to their sol-gel counterparts. This enhanced catalytic performance observed in the precipitation-derived nanoparticles was ascribed to their surface-active qualities [16]. Punitha and colleagues (2022) demonstrated that aluminium nanoparticles, synthesised using an extract from Citrus aurantium peel, exhibited a photocatalytic degradation efficiency of 89.1% for methylene blue herbicides [17]. Other studies also demonstrated the role of aluminium nanoparticles in the photocatalytic oxidation of organic compounds [18], [19]. This research gives insight that nanoparticles exhibit a high surface area-to-volume ratio, which enhances their catalytic activity and efficiency in oxidation reactions. When exposed to illumination, aluminium nanoparticles can generate reactive oxygen species (ROS), such as hydroxyl radicals and superoxide anions, which are powerful oxidising agents capable of degrading various organic pollutants.

In reusability studies, it was found that herbicide degradation efficiency was found to have reduced by 37% after five consecutive cycles, marking the catalyst re-usage up to five cycles (Fig. 7 and Table 3). Fig. 6 shows the kinetic fit for the degradation of ametryn by photocatalytic oxidation with aluminium nanoparticles as a catalyst [20-22]. The rate of reaction is dependent on the pollutant concentration since ametryn first adsorbs onto nanoparticles before the reaction. This adsorption-desorption reaches a dynamic equilibrium, and kinetic studies show that the pseudo-first-order rate kinetic model fits the process. The present study claims the degradation of ametryn to 84% with 2.5g/L of Al_2O_3 NP catalyst dosage, targeting 5 mg/L of initial herbicide concentration at pH 3.0 within 120 minutes of treatment duration under the illumination of UV light at an intensity of 5.6 mW/cm^2.

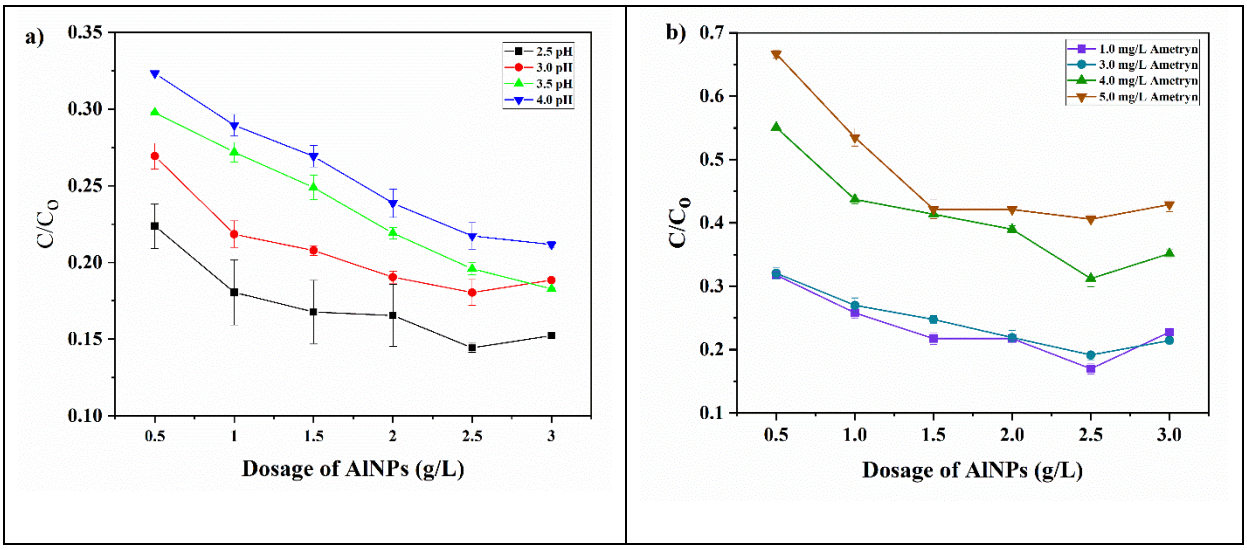

Fig. 6. Degradation of ametryn with different dosages of Al_2O_3 NPs at different a) pH and b) Initial concentration of ametryn

Table 2. Photocatalytic Degradation of Ametryn using Al_2O_3 NPs

Catalyst	Dosage of Nanoparticles (g/L)	Ametryn Degradation (%)	k	R^2
Aluminum Oxide Nanoparticles	0.5	67.32	0.00125	0.9446
	1.0	70.95	0.00083	0.9742
	1.5	77.53	0.00087	0.9811
	2.0	78.05	0.00078	0.9857
	2.5	84.00	0.00301	0.8904
	3.0	83.73	0.00240	0.9130

J Water Environ Nanotechnol, 2026, 11(3): 420-430
10.22090/jwent.2026.2076641.1997

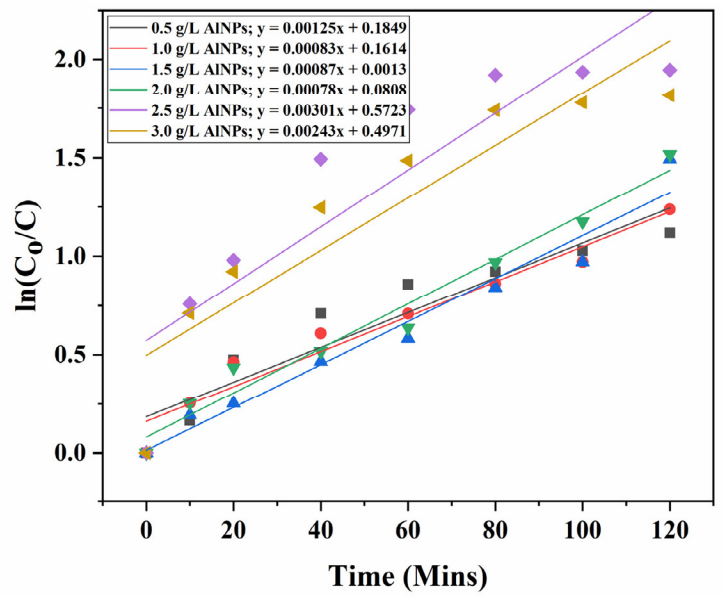

Fig. 7. Linear fit for the degradation of ametryn with different dosages of Al_2O_3 NPs

Table 3. Reusability of Al_2O_3 NPs in photocatalytic degradation of ametryn

Catalyst	Dosage of Nanoparticles (g/L)	Reuse	Ametryn Degradation (%)
Aluminum Oxide Nanoparticles	2.5	Cycle1	82.97
		Cycle2	78.68
		Cycle3	73.69
		Cycle4	67.59
		Cycle5	47.88

3.4 Mechanism of photo-catalytic degradation of Ametryn

Photodegradation through photocatalytic oxidation involves the activation of a photocatalyst, such as aluminium oxide nanoparticles (Al_2O_3 NPs), under ultraviolet (UV) light, initiating a series of photo-induced redox reactions. When Al_2O_3 NPs absorb photons matching their localized surface plasmon resonance, electrons in the valence band are excited to the conduction band, generating electron-hole pairs. These charge carriers interact with water and oxygen molecules adsorbed on the nanoparticle surface to produce reactive oxygen species (ROS), primarily hydroxyl radicals (•OH) and superoxide anions ($O_2^{\bullet-}$). The highly reactive hydroxyl radicals attack the adsorbed organic pollutant molecules, such as ametryn herbicide, breaking down their complex chemical structures into smaller, less harmful compounds. The adsorption of ametryn onto the negatively charged AlNP surface (zeta potential of -25.9 mV) is enhanced under acidic conditions due to electrostatic attraction with positively charged ametryn molecules, facilitating proximity for effective radical-mediated oxidation.

The kinetic behavior implies that the degradation rate is directly proportional to the concentration of ametryn molecules adsorbed on the surface of the catalyst, as the reaction follows pseudo-first-order kinetics. The adsorption step is critical, as it governs the availability of pollutant molecules in proximity to reactive sites where oxidative reactions occur. Increasing the catalyst dosage effectively raises the number of active sites on the Al_2O_3 NPs surface available for the generation of reactive oxygen species (ROS), such as hydroxyl radicals (•OH) and superoxide anions ($O2^{\bullet-}$). These ROS are the primary oxidizing agents responsible for breaking down the ametryn molecules. As the catalyst loading increases, more electron-hole pairs are generated upon UV illumination, leading to enhanced ROS production and thus higher degradation efficiency. This is evidenced by the observed increase in degradation percentage with catalyst dosages ranging from 0.5 g/L to 3.0 g/L.

However, at higher initial concentrations of ametryn, the catalyst surface active sites may become saturated. This saturation limits the adsorption capacity, reducing the effective contact between ametryn molecules and ROS. Consequently,

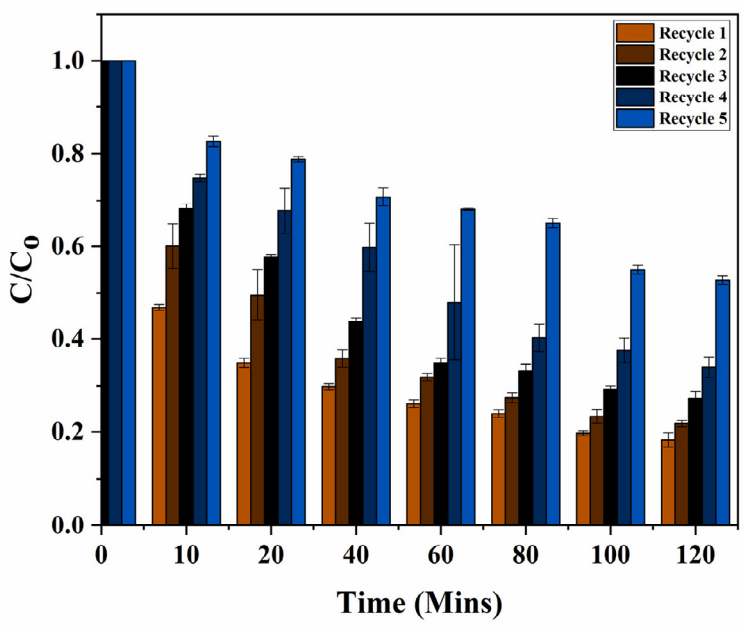

Fig. 8. Reusability Studies of Al_2O_3 NPs on ametryn Degradation.

Table 4. Comparison of photocatalytic degradation of different organic pollutants using aluminum nanoparticles with previous studies

Catalyst	Target compound	Percentage removal	Catalyst dosage	Reference
Al- doped Nano TiO_2	Organic pollutants from wastewater	75%	2g	[3]
Al_2O_3 NPs	Methylene blue	85%	10mg	[2]
Al_2O_3 NPs	Methylene blue	99.2%	10mg	[24]
Al_2O_3 NPs	Malachite green dye	45%	100mg	[22]
Al_2O_3 NPs	Azo dye	36%	30mg	[11]
Al_2O_3 NPs	Ametryn	84%	2.5g	Present study

the degradation rate diminishes despite the presence of sufficient ROS, as fewer pollutant molecules are accessible for oxidation. This competitive adsorption and site saturation explain the decline in degradation efficiency at elevated pollutant concentrations. Structurally, the aluminium oxide framework of the nanoparticles demonstrates stability throughout the photodegradation process. FTIR analyses confirm that the core aluminium oxide lattice remains intact after repeated use, maintaining the catalyst's fundamental properties. This structural robustness allows for catalyst recovery and reuse over multiple cycles. The degradation efficiency decreases progressively with each reuse cycle, showing a 37% reduction after five cycles. This decline is attributed primarily to surface fouling, accumulation of degradation intermediates or adsorbed species that block active sites, and minor structural changes that may slightly alter surface properties or reduce active site availability.

4. CONCLUSIONS

The phytochemical synthesis of green aluminium oxide nanoparticles resulted in the formation of agglomerated spherical nanoparticles, as confirmed by energy-dispersive X-ray Spectroscopy (EDS) and X-ray Diffraction (XRD) studies. These synthesised nanoparticles demonstrated significant catalytic activity in photochemical oxidation processes, achieving a maximum herbicide removal efficiency of 84.0% within 120 minutes of treatment. The effectiveness of the oxidation process was further evidenced by a substantial Chemical Oxygen Demand (COD) removal of 74.2% within the same timeframe, indicating improved oxidation during the treatment process. The performance of the nanoparticles was influenced by the initial concentration of ametryn herbicides. An increase in the initial herbicide concentration from 5 mg/L to 20 mg/L led to a 23.5% decrease in degradation efficiency, highlighting the impact of herbicide concentration on the

J Water Environ Nanotechnol, 2026, 11(3): 420-430
10.22090/jwent.2026.2076641.1997

treatment process. Importantly, recoverability and reusability studies demonstrated that the nanoparticles could be effectively reused for up to five consecutive cycles in the removal of ametryn, suggesting their potential for sustainable and cost-effective application in water treatment processes.

Consent to publish
The authors have consent to publish this article.

Conflict of Interest
The authors have no competing interests to declare that are relevant to the content of this article..

Funding
No funding was received for conducting this study.

Author's Contributions
Study Conception or Design: Kavya B.M., T. Mahadevaiah
Data Acquisition: Kavya B.M., T. Mahadevaiah
Data Analysis or Interpretation: Kavya B.M., T. Mahadevaiah
Manuscript Drafting: Kavya B.M., T. Mahadevaiah
Critical Manuscript Revision: Kavya B.M., T. Mahadevaiah
All authors have approved the final manuscript and are responsible for all aspects of the work.

AI Statement
The authors confirm that no AI tools or services were used during the preparation of this work.

Availability of data and materials
No data availability for this study.

REFERENCES

1. Ali NS, Kalash KR, Ahmed AN, Albayati TM. Performance of a solar photocatalysis reactor as pretreatment for wastewater via UV, UV/TiO2, and UV/H2O2 to control membrane fouling. Sci Rep. 2022;12(1):1-10. https://doi.org/10.1038/s41598-022-20984-0
2. Anna KK, Bogireddy NKR, Agarwal V, Bon RR. Synthesis of α and γ phase of aluminium oxide nanoparticles for the photocatalytic degradation of methylene blue under sunlight: A comparative study. Mater Lett. 2022;317:132085. https://doi.org/10.1016/j.matlet.2022.132085
3. Areerachakul N, Sakulkhaemaruethai S, Johir MAH, Kandasamy J, Vigneswaran S. Photocatalytic degradation of organic pollutants from wastewater using aluminium doped titanium dioxide. J Water Process Eng. 2019;27:177-184. https://doi.org/10.1016/j.jwpe.2018.12.006
4. Bahrami S, Ahmadpour A, Bastami TR, Ayati A, Mirzaei S. Comparative study of metal nanoparticles anchored TiO2 using polyoxometalate intermediate in photodegradation of azo dye pollutant in aquatic environments. Inorg Chem Commun. 2024;160:111986. https://doi.org/10.1016/j.inoche.2023.111986
5. Bhaskar S, Manu B, Sreenivasa MY. Bioleached laterite nano iron catalyst (BLaNFeCs)-based Fenton's degradation of selective dyes in water. H2Open J. 2022;5(3):382-393. https://doi.org/10.2166/h2oj.2022.045
6. Bokare AD, Choi W. Review of iron-free Fenton-like systems for activating H2O2 in advanced oxidation processes. J Hazard Mater. 2014;275:121-135. https://doi.org/10.1016/j.jhazmat.2014.04.054
7. Boussahel R, Harik D, Mammar M, Lamara-mohamed S. Degradation of obsolete DDT by Fenton oxidation with zero-valent iron. Desalination. 2007;206(1-3):369-372. https://doi.org/10.1016/j.desal.2006.04.059
8. Chen F, Xie S, Huang X, Qiu X. Ionothermal synthesis of Fe3O4 magnetic nanoparticles as efficient heterogeneous Fenton-like catalysts for degradation of organic pollutants with H2O2. J Hazard Mater. 2017;322:152-162. https://doi.org/10.1016/j.jhazmat.2016.02.073
9. Davarpanah M, Ahmadpour A, Bastami TR. Preparation and characterization of anion exchange resin decorated with magnetite nanoparticles for removal of p-toluic acid from aqueous solution. J Magn Magn Mater. 2015;375:177-183. https://doi.org/10.1016/j.jmmm.2014.09.065
10. Davarpanah M, Ahmadpour A, Rohani-Bastami T, Dabir H. Synthesis and application of diethanolamine-functionalized polystyrene as a new sorbent for the removal of p-toluenesulfonic acid from aqueous solution. J Ind Eng Chem. 2015;30:281-288. https://doi.org/10.1016/j.jiec.2015.05.034
11. Dhawale VP, Khobragade V, Kulkarni SD. Synthesis and characterization of aluminium oxide (Al2O3) nanoparticles and its application in azo dye decolourisation. Chemistry. 2018;27(1):31-37.
12. AlHamedi FH, Rauf MA, Ashraf SS. Degradation studies of Rhodamine B in the presence of UV/H2O2. Desalination. 2009;239(1-3):159-166. https://doi.org/10.1016/j.desal.2008.03.016
13. Franson MAH. Standard Methods for the Examination of Water and Wastewater. American Public Health Association; 1992.
14. Huang CP, Dong C, Tang Z. Advanced Chemical Oxidation: Its Present Role And Potential Future In Hazardous Waste Treatment. 1993. https://doi.org/10.1016/0956-053X(93)90070-D
15. Iervolino G. Visible light active photocatalysts for the removal of inorganic emerging contaminants. In: Emerging Contaminants in the Environment. Elsevier; 2020. https://doi.org/10.1016/B978-0-12-818334-2.00006-7
16. Jaafarzadeh N, Kakavandi B, Takdastan A. Powder activated carbon/Fe3O4 hybrid composite as a highly efficient heterogeneous catalyst for Fenton oxidation of tetracycline: degradation mechanism and kinetic. RSC Adv. 2015;5(103):84718-84728. https://doi.org/10.1039/C5RA17953J
17. Kang S, Liu S, Wang H, Cai W. Enhanced degradation performances of plate-like micro/nanostructured zero valent iron to DDT. J Hazard Mater. 2016;307:145-153. https://doi.org/10.1016/j.jhazmat.2015.12.063
18. Kumar Anna K, Kumar Reddy Bogireddy N, Agarwal V, Ramírez Bon R. Synthesis of α and γ phase of aluminium oxide nanoparticles for the photocatalytic degradation of methylene blue under sunlight: A comparative study. Mater Lett. 2022;317:132085. https://doi.org/10.1016/j.matlet.2022.132085
19. Li H, Zhu J, Xiao P, et al. On the mechanism of oxidative degradation of rhodamine B over LaFeO3 catalysts supported on silica materials: Role of support. Microporous Mesoporous Mater. 2016;221:159-166. https://doi.org/10.1016/j.micromeso.2015.09.034
20. Malgwi DW, Musa C, Aminu A. Photocatalytic activity of biosynthesized aluminium oxide nanoparticle from leaves of Prosopis africana plant. J Res Chem. 2024;5(2):122-128.
21. Nagarajan P, Subramaniyan V, Elavarasan V, et al. Biofabricated

Aluminium Oxide Nanoparticles Derived from Citrus aurantium L.: Antimicrobial, Anti-Proliferation, and Photocatalytic Efficiencies. Sustainability. 2023;15(2):1743. https://doi.org/10.3390/su15021743

22. Pathania D, Katwal R, Kaur H. Enhanced photocatalytic activity of electrochemically synthesized aluminum oxide nanoparticles. Int J Miner Metall Mater. 2016;23(3):358-371. https://doi.org/10.1007/s12613-016-1245-9
23. Ribeiro JP, Cruz NC, Neves MC, et al. Granulated biomass fly ash coupled with fenton process for pulp and paper wastewater treatment. Environ Pollut. 2023;317:120777. https://doi.org/10.1016/j.envpol.2022.120777
24. Sharma B, Sahi A, Dhau J, Kaushik A, Kumar R, Chaudhary GR. Recycling waste aluminium foil to bio-acceptable nano photocatalysts [aluminium oxide (Al2O3) & aluminium oxyhydroxide (AlOOH)]; dye degradation as proof-of-concept. Mater Adv. 2024;5(20):8304-8317. https://doi.org/10.1039/D4MA00717D
25. Segura Y, Martínez F, Melero JA, et al. Enhancement of the advanced Fenton process (Fe0/H2O2) by ultrasound for the mineralization of phenol. Appl Catal B Environ. 2012;113-114:100-106. https://doi.org/10.1016/j.apcatb.2011.11.024
26. Su S, Guo W, Leng Y, et al. Heterogeneous activation of Oxone by CoxFe3−xO4 nanocatalysts for degradation of rhodamine B. J Hazard Mater. 2013;244-245:736-742. https://doi.org/10.1016/j.jhazmat.2012.11.005
27. U EA, C NE, C OC, et al. Photocatalytic Activity of Aluminium Oxide Nanoparticles on Degradation of Ciprofloxacin. Saudi J Eng Technol. 2022;7(3):132-136. https://doi.org/10.36348/sjet.2022.v07i03.003
28. Zhou W, Zhao H, Gao J, et al. Influence of a reagents addition strategy on the Fenton oxidation of rhodamine B: control of the competitive reaction of .OH. RSC Adv. 2016;6(109):108791-108800. https://doi.org/10.1039/C6RA20242J